Electronic Supplementary Information

Water-Soluble Conjugated Polyelectrolyte for Selective and Sensitive Detection of Carcinogenic Chromium(VI)

Arvin Sain Tanwar,[a,b] Mst Nasima Khatun,[a] Moirangthem Anita Chanu,[a] Tapshi Sarmah,[a] Yeon-Ho Im, [b*] and Parameswar Krishnan Iyer[a,c*]

[a]Department of Chemistry, Indian Institute of Technology Guwahati, Guwahati 781039, India.

[b]School of Semiconductor and Chemical Engineering, Clean Energy Research Center, Jeonbuk National University, Jeonju, Jeonbuk 54896, Republic of Korea.

[c]Centre for Nanotechnology, Indian Institute of Technology Guwahati, Guwahati, 781039, India

AUTHOR EMAIL ADDRESS: pki@iitg.ernet.in; yeonhoim@jbnu.ac.kr

AUTHOR FAX: +91 361 258 2349

Table S1: A comparative study of few optical sensors recently developed for detection of Cr(VI).

Material Used	Detection Limit	Sensing Mechanism	Quenching Constant (M^{-1})	Reference
Conjugated Polyelectrolyte (PPMI)	*0.85×10^{-9} M (0.250 ppb)*	*Static Quenching*	*1.32×10^{6}*	*This work*
MA-1@CNT-NB	76.9×10^{-9} M	IFE	1.0×10^{5}	1
MOF based	1 ppb in 5 to 10 min	Absorbance @395 nm	-	2
Cotton Fabric	0.029 mg/L in 30 s & 0.0013 mg/L in 5 min	Colorimetric	-	3
MWCNs nanozymes	40×10^{-9} M	Colorimetric	-	4
Cal-CS/PEG/Ag nanohybrids	79×10^{-9} M	Colorimetric	-	5
MOF	0.09×10^{-6} M	IFE	2.00×10^{4}	6
nanoparticles	0.03×10^{-6} M	Colorimetric	-	7
MOF	0.33×10^{-6} M	RET	1.32×10^{4}	8
Polyfluorene P(Fmoc-Arg-OH) and P(Fmoc-GluOH)	0.016×10^{-9} M and 3.33×10^{-6} M	-	-	9
acridine-diphenylacetyl moiety (NDA)	0.160×10^{-6} M	Complexation ("ICT OFF")	-	10
MOF	18×10^{-9} M	IFE	-	11
MOF	20×10^{-9} M	Electron transfer	-	12
Nanocomposite	66×10^{-9} M	PET	2.99×10^{5}	13
Carbon dots-wrapped Boehmite nanoparticles	58×10^{-9} M	PET	1.75×10^{5}	14
CB[6]-based supramolecular assembly	3.9×10^{-6} M	FRET	6×10^{3}	15
gold nanoclusters	0.12×10^{-6} M	-	13.28 ppm^{-1}	16
MOF	0.41×10^{-6} M	Absorbance of excitation light (pIFE)	1.38×10^{4}	17
Non-conjugated polymer (GCPF)	0.22×10^{-6} M	Oxidative damage to (GCPF)	-	18
nanocomposite	1 ppb	Electron transfer	-	19
MOF	-	-	9.19×10^{5}	20
MOF	3.53×10^{-6} M	Electronic interactions	2.07×10^{4}	21

Table S2: Fluorescence lifetime decay of each component and their fractions of PPMI in presence of different amounts of Cr(VI).

Sample	τ_1 (ns)	%	τ_2 (ns)	%	τ_3 (ns)	%	χ^2	τ_{avg} (ns)
PPMI	1.208	52.58	4.025	47.41	-	-	0.944	2.54
PPMI + Cr(VI) (3.33 µM)	0.570	24.08	1.914	37.94	5.093	37.97	1.016	2.79
PPMI + Cr(VI) (6.66 µM)	0.560	6.93	1.791	40.24	5.158	52.81	1.073	3.48
PPMI + Cr(VI) (10.0 µM)	0.272	16.42	1.582	37.66	5.186	45.91	1.017	3.02

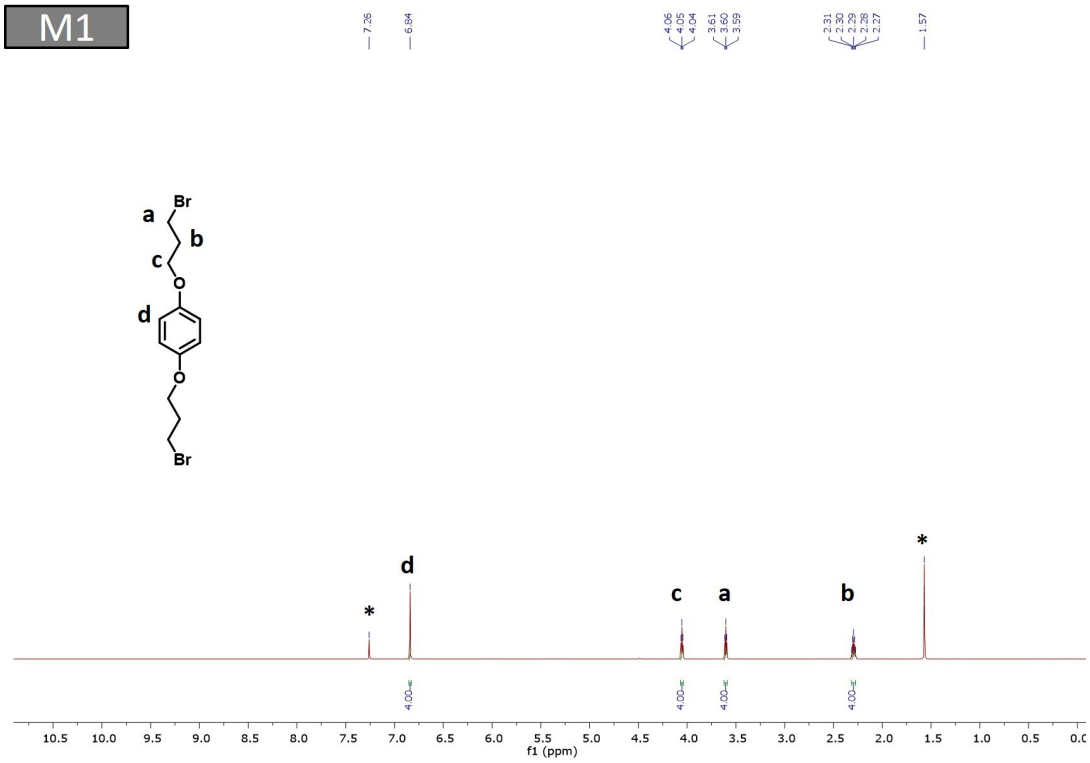

Fig. S1 ^{1}H NMR spectra of M1.

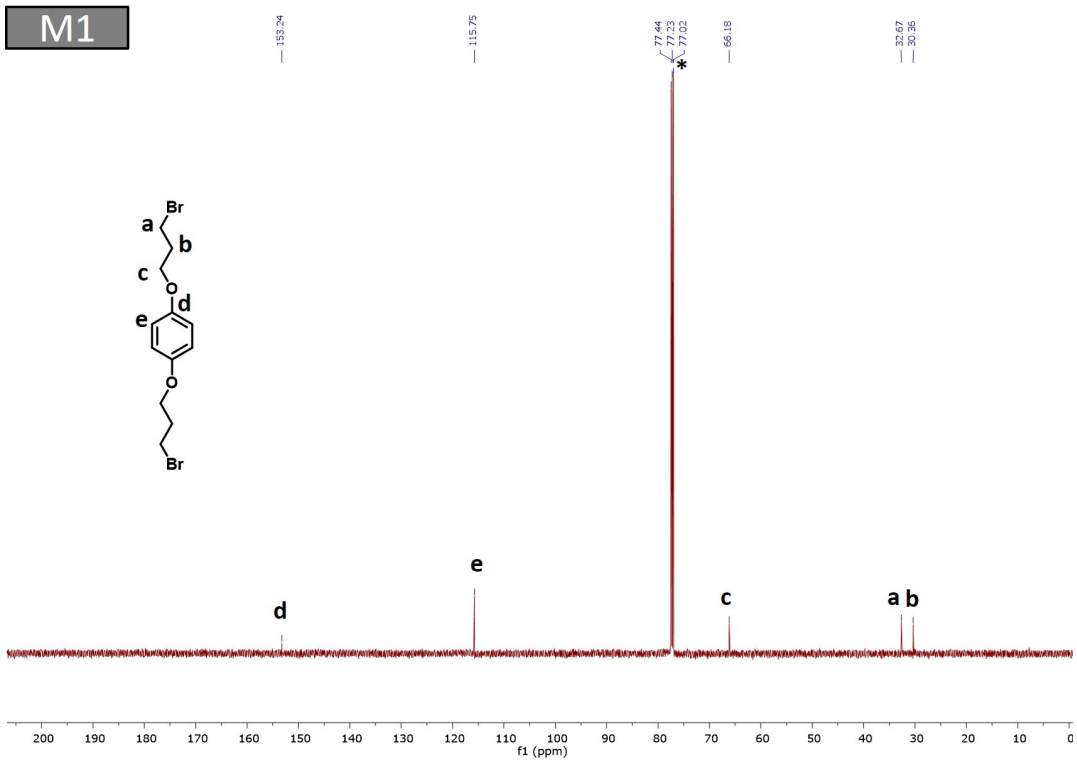

Fig. S2 ^{13}C NMR spectra of M1.

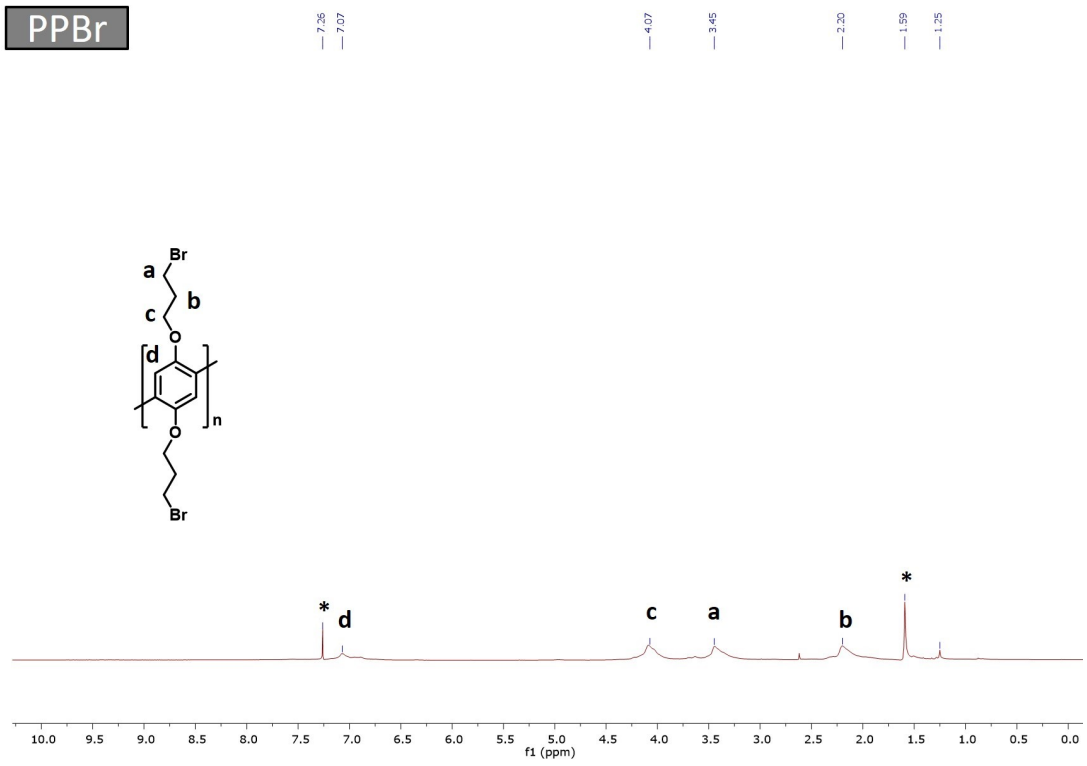

Fig. S3 ^{1}H NMR spectra of PPBr.

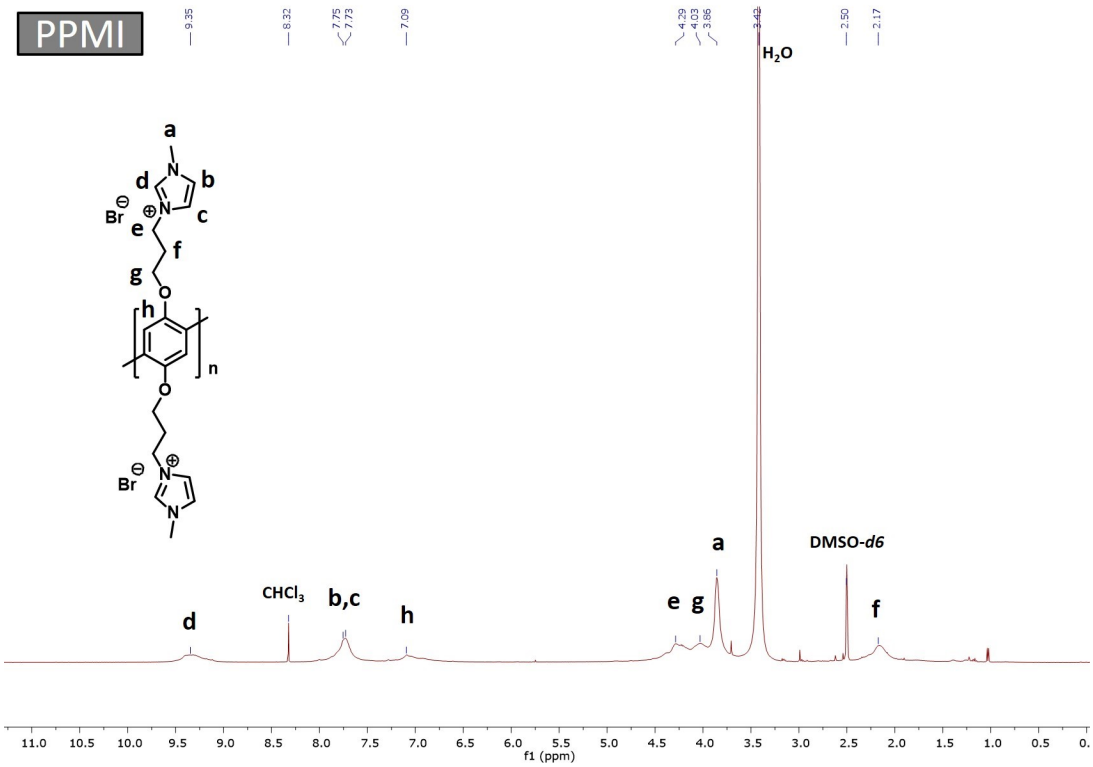

Fig. S4 ^{1}H NMR spectra of PPMI.

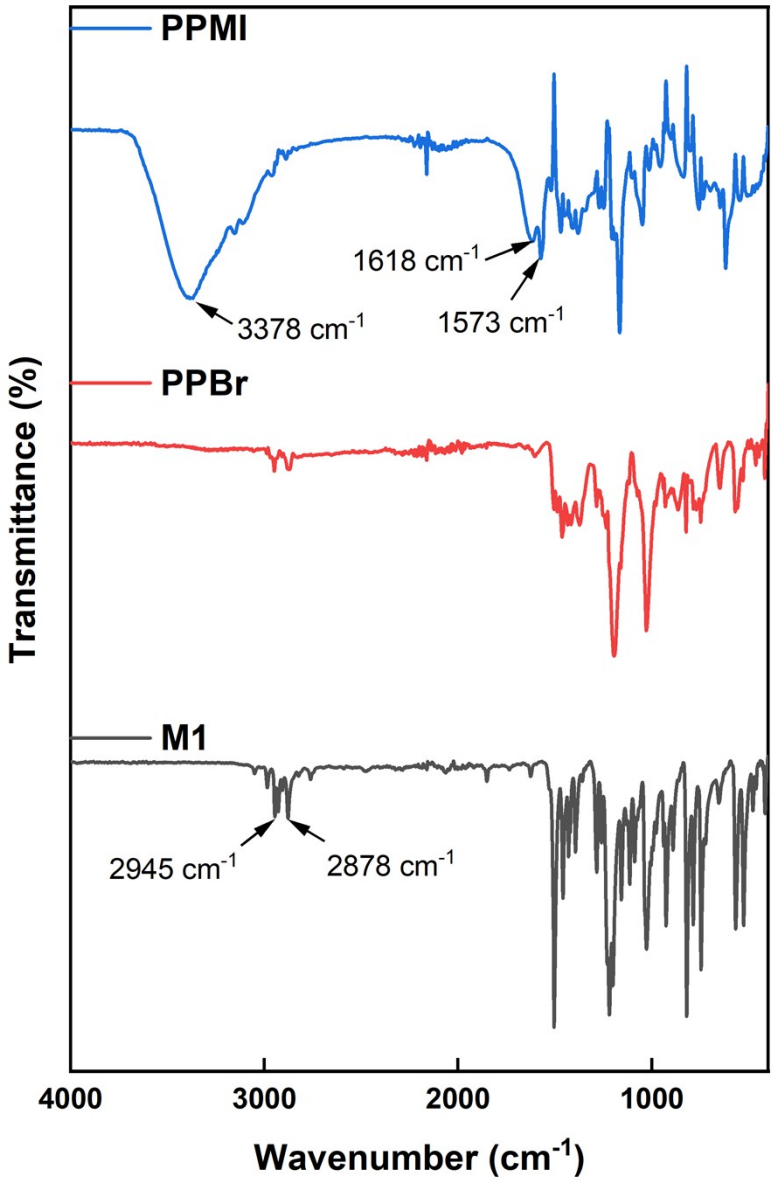

Fig. S5 FTIR spectra of M1, PPBr and PPMI.

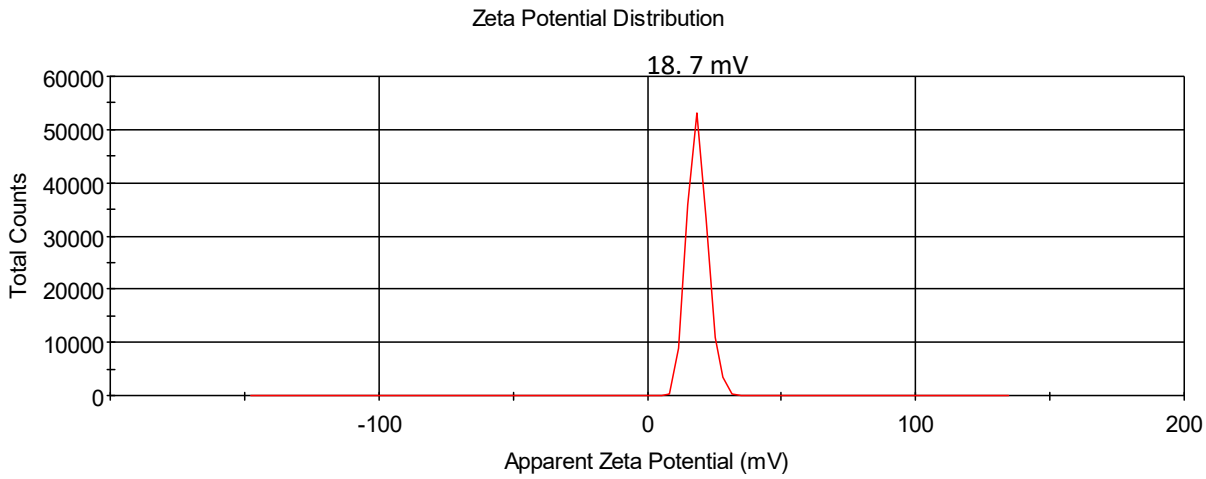

Fig. S6. Zeta potential of PPMI.

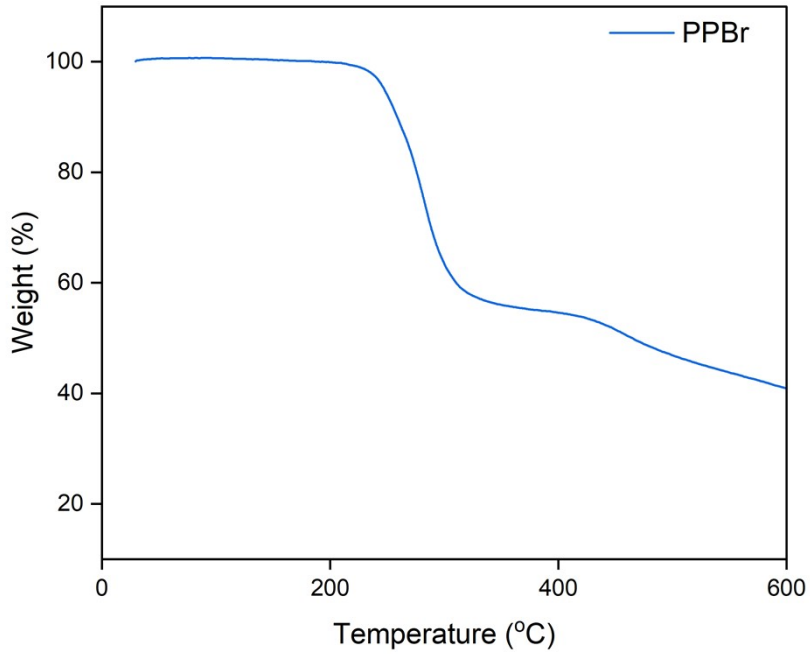

Fig. S7. TGA of PPBr (~2.1 mg, 10°C/min, 0-600 °C).

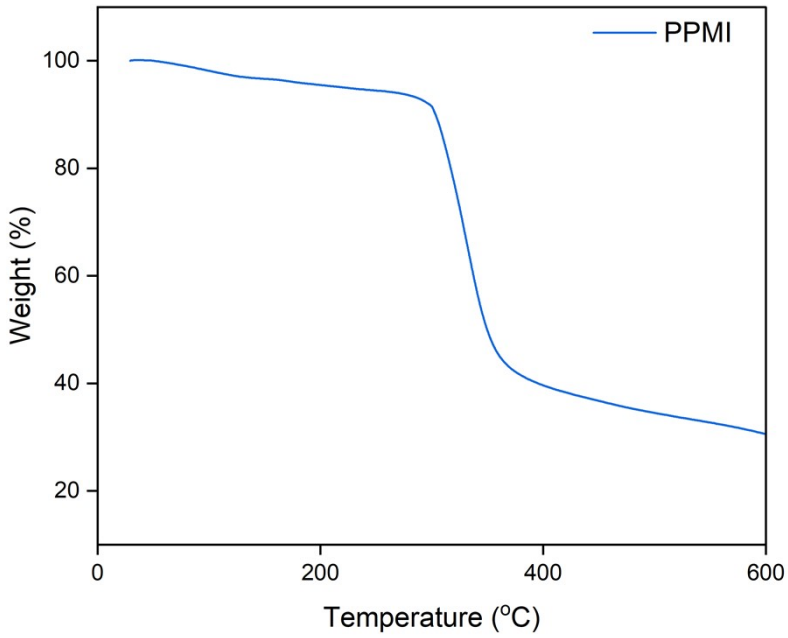

Fig. S8. TGA of PPMI (~3.9 mg, 10°C/min, 0-600 °C).

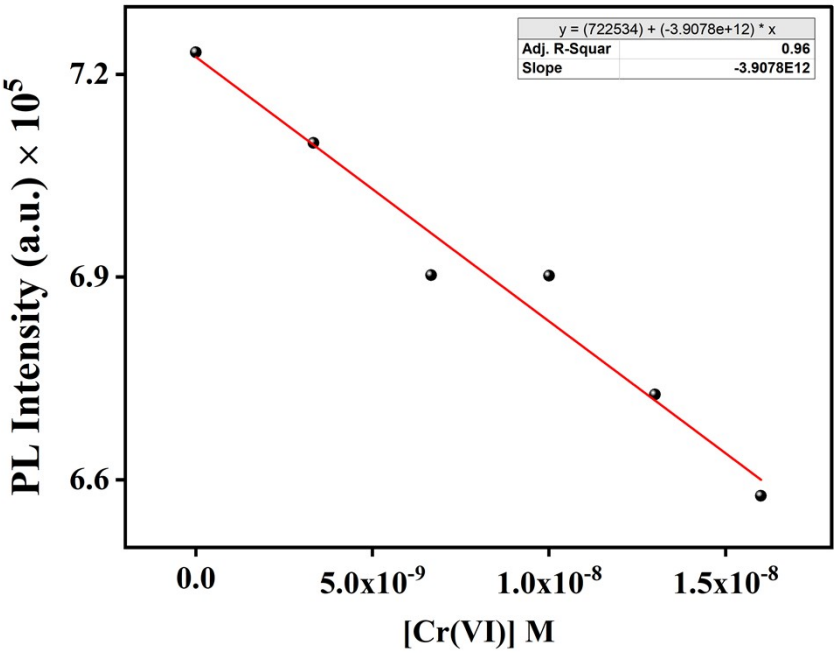

Fig. S9 Fluorescence intensity of PPMI *vs* Cr(VI) concentration.

LOD = 3 × S.D./k

LOD = 3 × 1113.56 / (3.91×10^{12})

LOD = 0.85 nM

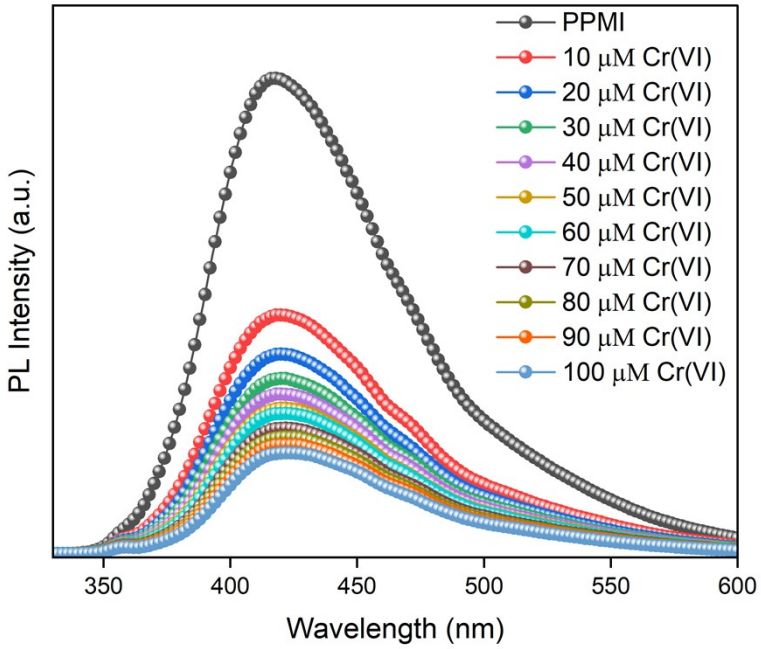

Fig. S10 Emission spectra of PPMI after the addition of different amounts of Cr(VI) in HEPES buffer (pH 7.2, 10 mM).

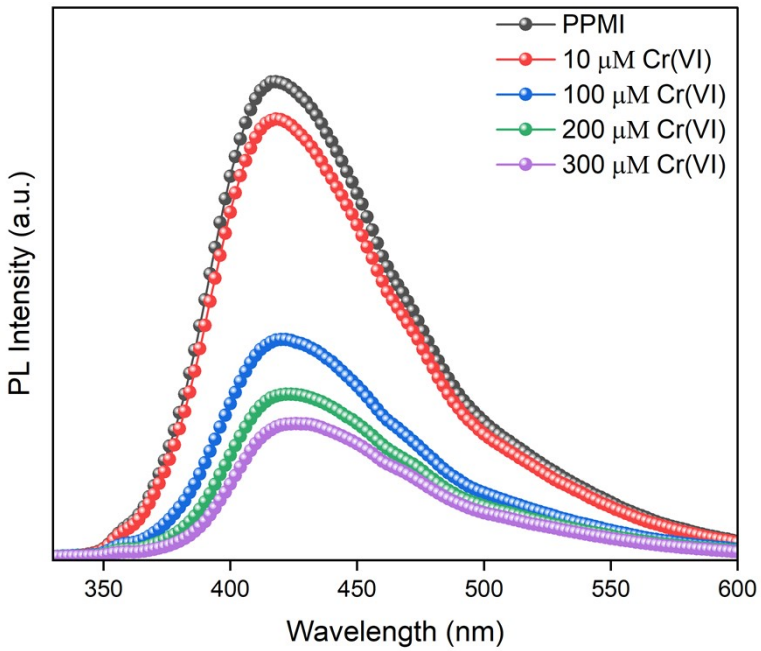

Fig. S11 Emission spectra of PPMI after the addition of different amounts of Cr(VI) in PBS buffer (pH 7.2).

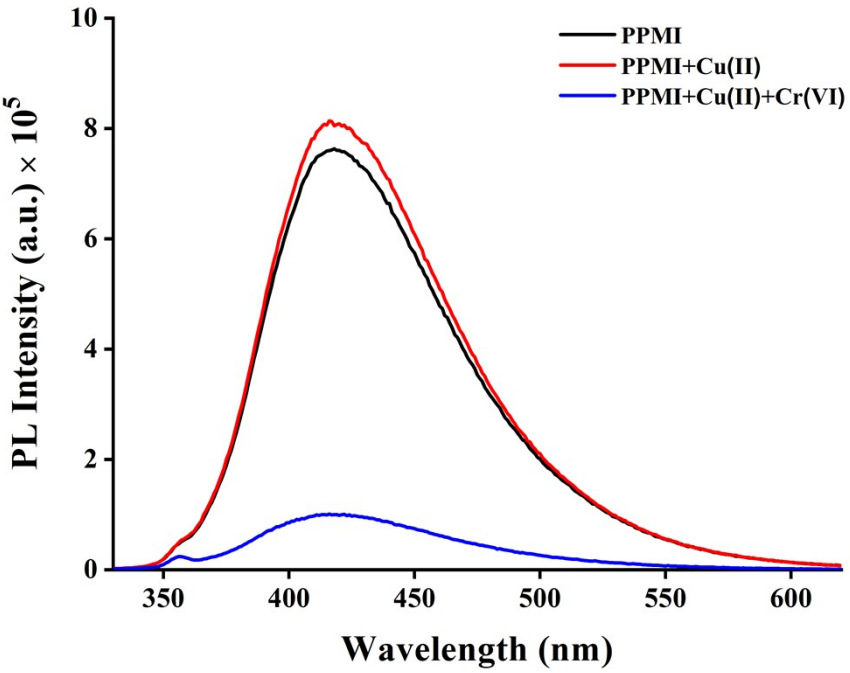

Fig. S12 Emission spectra of PPMI (black), PPMI in presence of Cu(II) (10 μM) (red), followed by addition of Cr(VI) (10 μM) (blue).

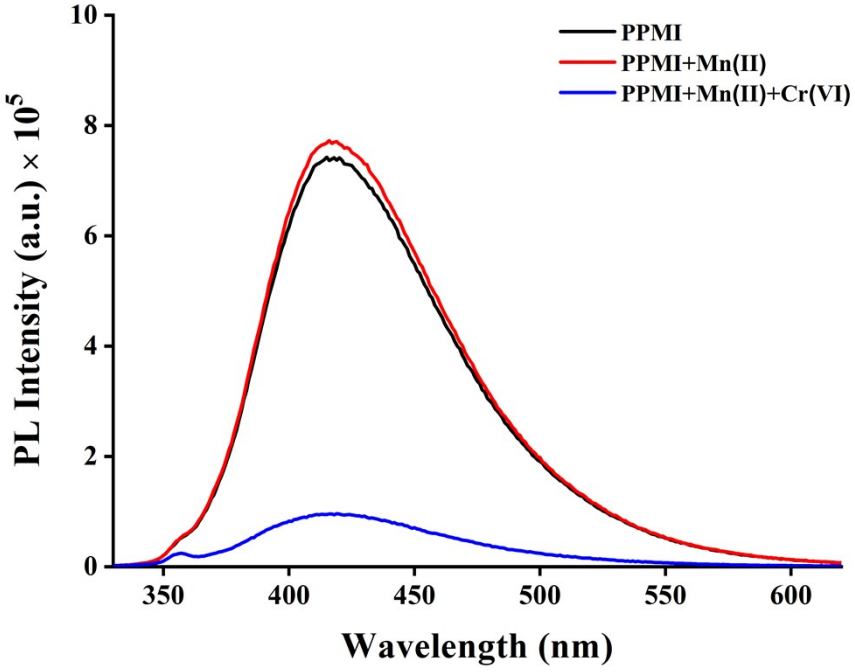

Fig. S13 Emission spectra of PPMI (black), PPMI in presence of Mn(II) (10 μM) (red), followed by addition of Cr(VI) (10 μM) (blue).

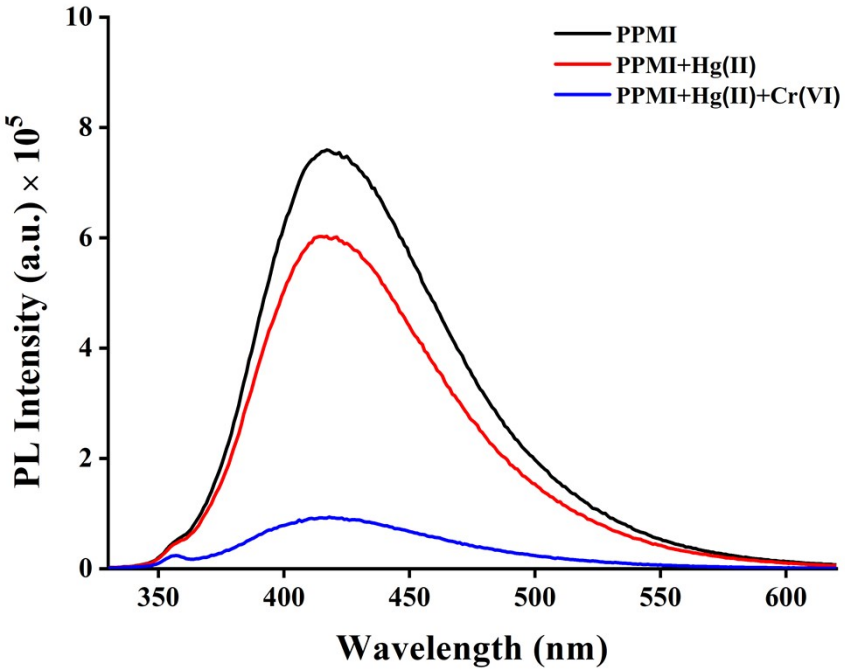

Fig. S14 Emission spectra of PPMI (black), PPMI in presence of Hg(II) (10 μM) (red), followed by addition of Cr(VI) (10 μM) (blue).

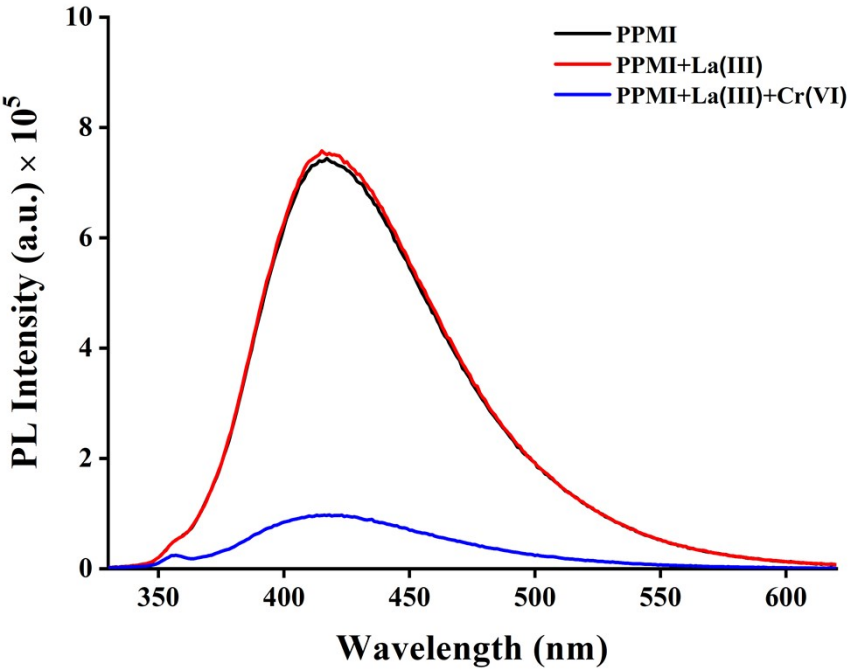

Fig. S15 Emission spectra of PPMI (black), PPMI in presence of La(III) (10 μM) (red), followed by addition of Cr(VI) (10 μM) (blue).

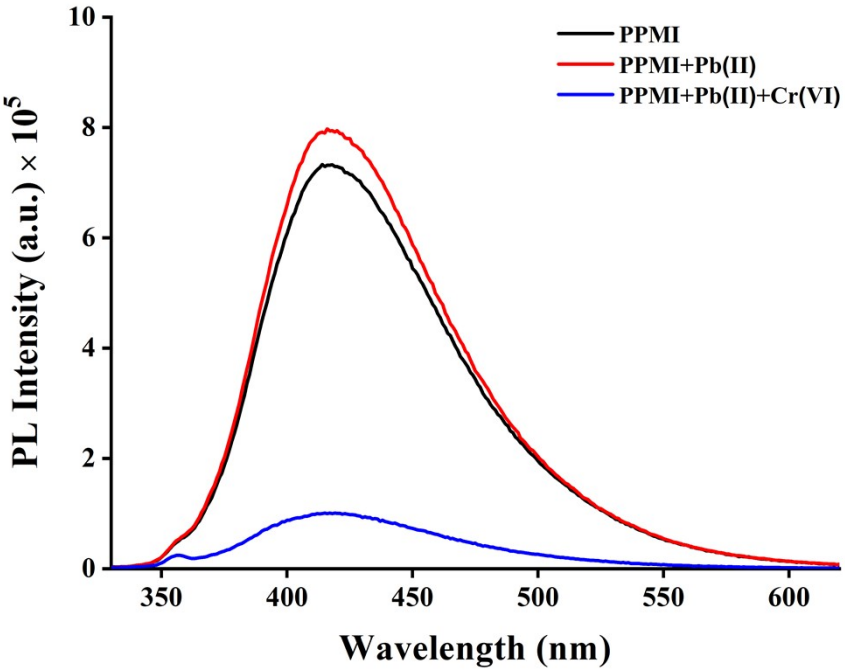

Fig. S16 Emission spectra of PPMI (black), PPMI in presence of Pb(II) (10 μM) (red), followed by addition of Cr(VI) (10 μM) (blue).

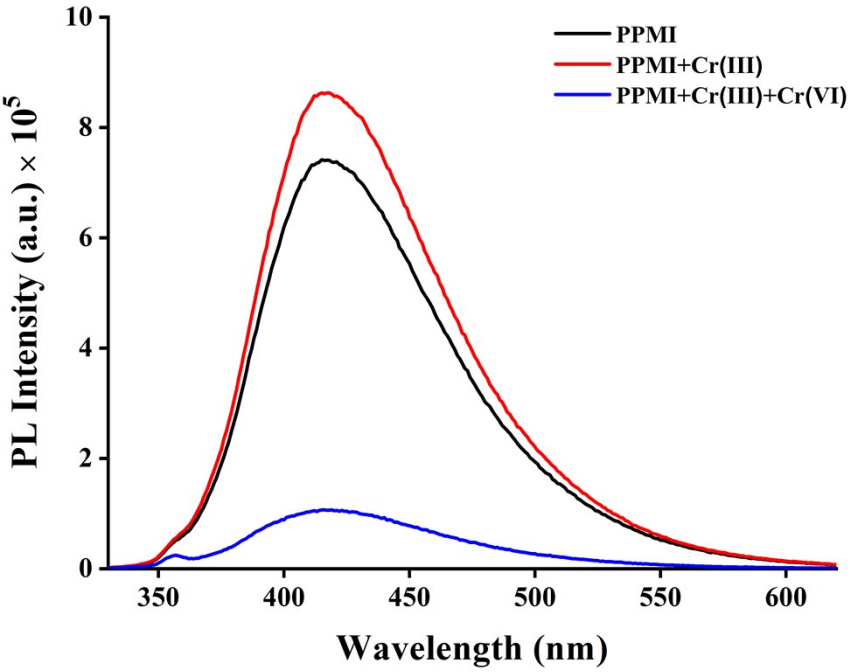

Fig. S17 Emission spectra of PPMI (black), PPMI in presence of Cr(III) (10 μM) (red), followed by addition of Cr(VI) (10 μM) (blue).

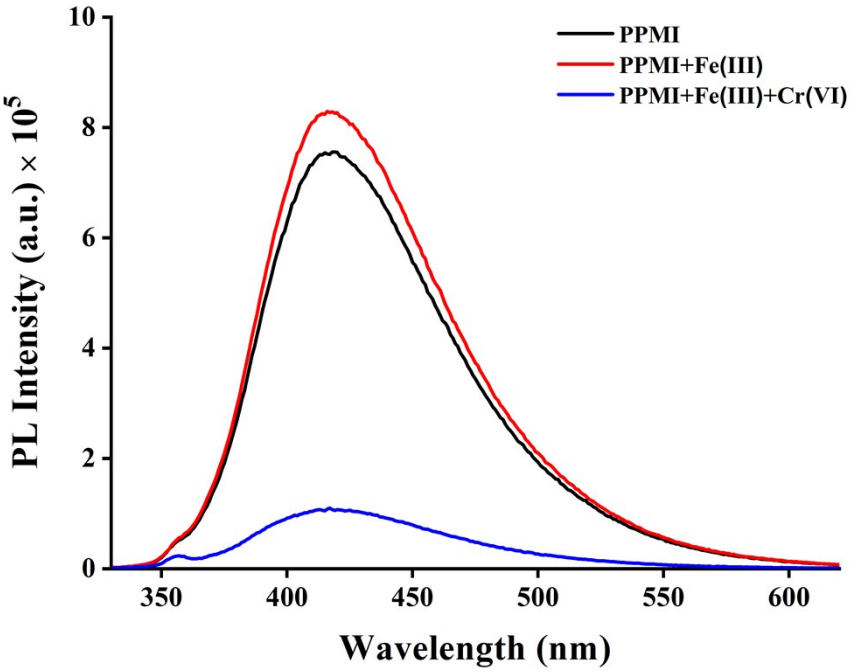

Fig. S18 Emission spectra of PPMI (black), PPMI in presence of Fe(III) (10 μM) (red), followed by addition of Cr(VI) (10 μM) (blue).

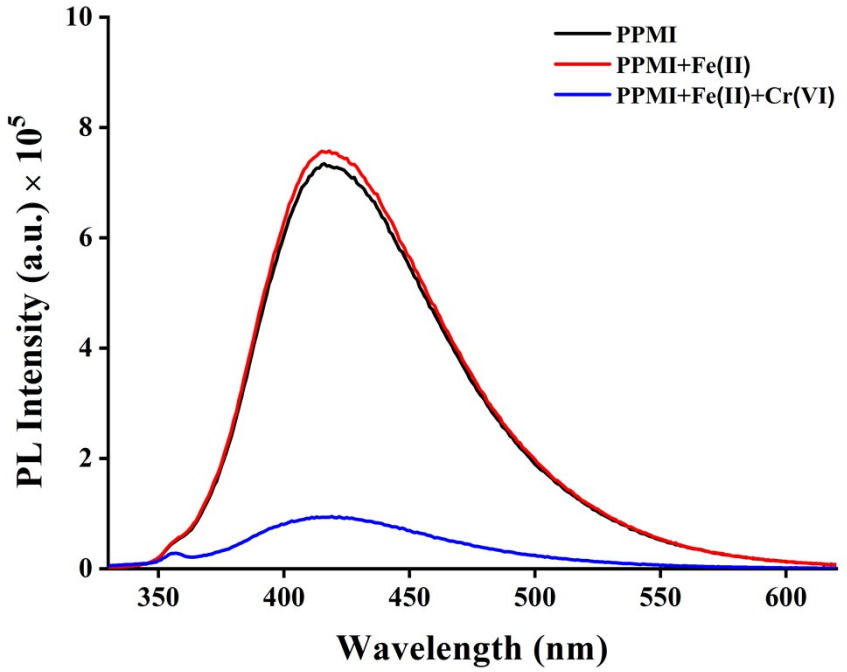

Fig. S19 Emission spectra of PPMI (black), PPMI in presence of Fe(II) (10 μM) (red), followed by addition of Cr(VI) (10 μM) (blue).

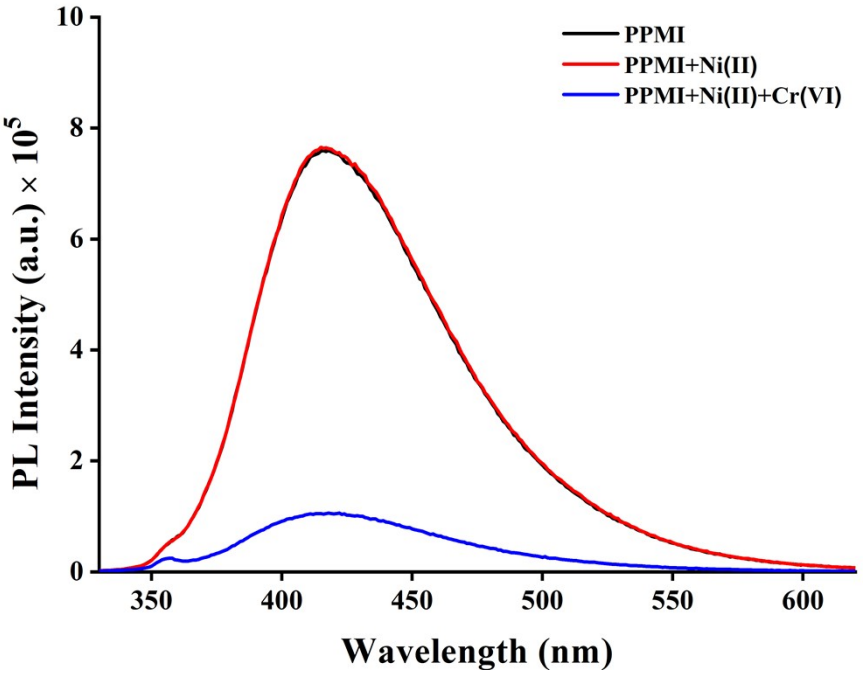

Fig. S20 Emission spectra of PPMI (black), PPMI in presence of Ni(II) (10 μM) (red), followed by addition of Cr(VI) (10 μM) (blue).

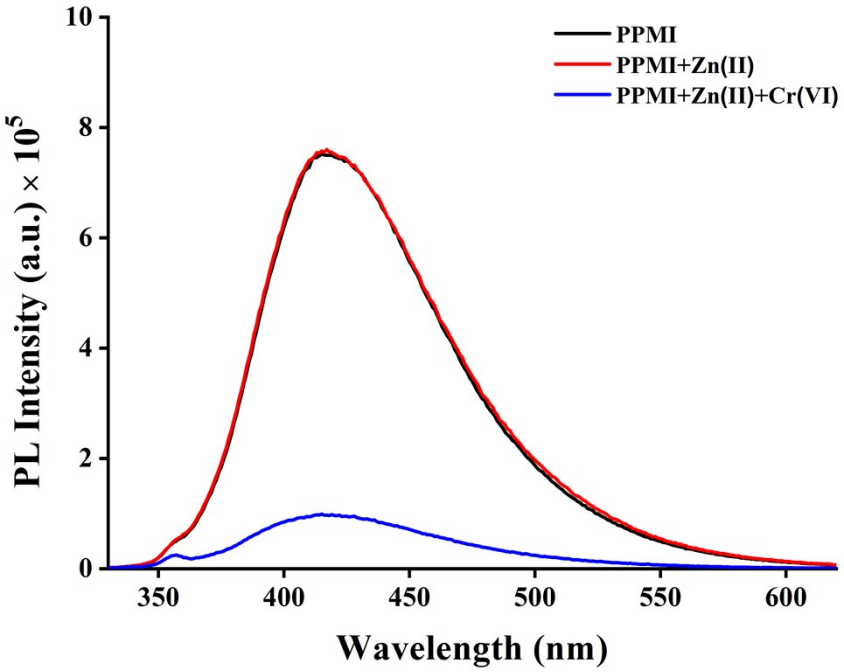

Fig. S21 Emission spectra of PPMI (black), PPMI in presence of Zn(II) (10 μM) (red), followed by addition of Cr(VI) (10 μM) (blue).

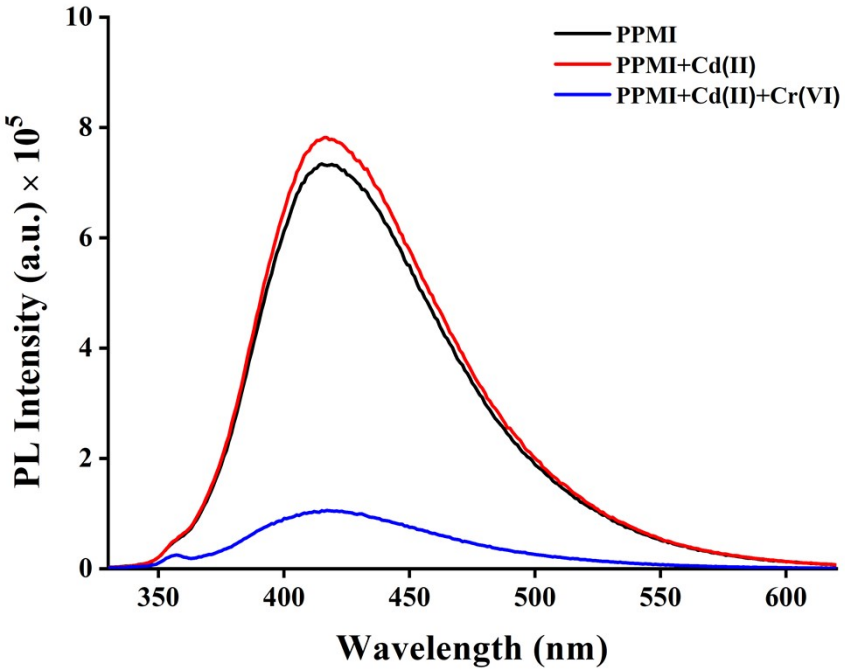

Fig. S22 Emission spectra of PPMI (black), PPMI in presence of Cd(II) (10 μM) (red), followed by addition of Cr(VI) (10 μM) (blue).

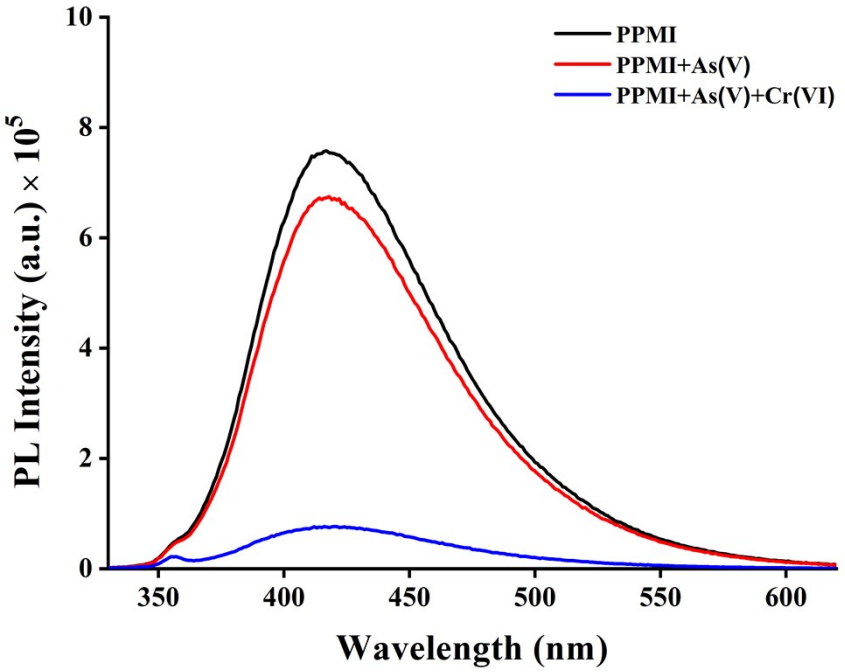

Fig. S23 Emission spectra of PPMI (black), PPMI in presence of As(V) (10 μM) (red), followed by addition of Cr(VI) (10 μM) (blue).

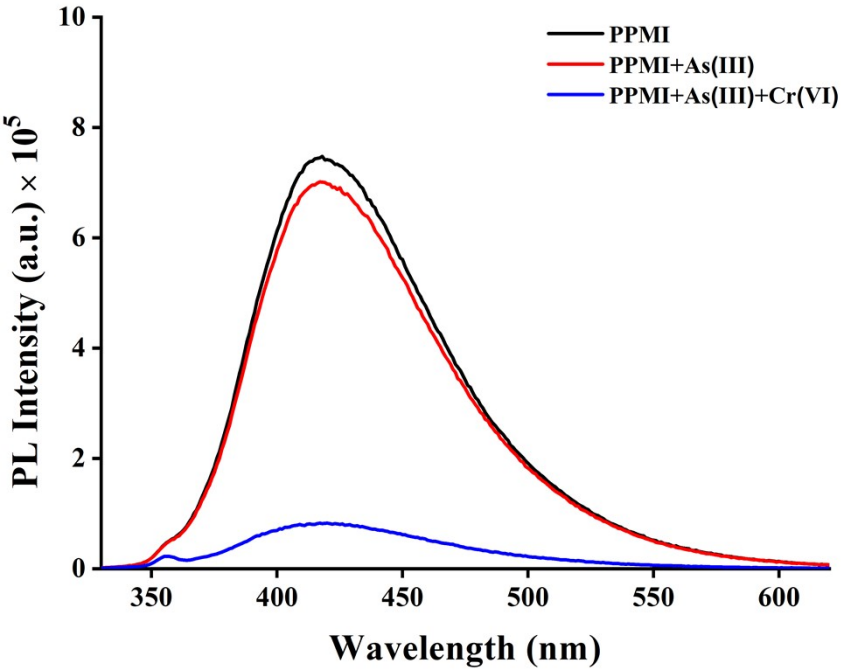

Fig. S24 Emission spectra of PPMI (black), PPMI in presence of As(III) (10 μM) (red), followed by addition of Cr(VI) (10 μM) (blue).

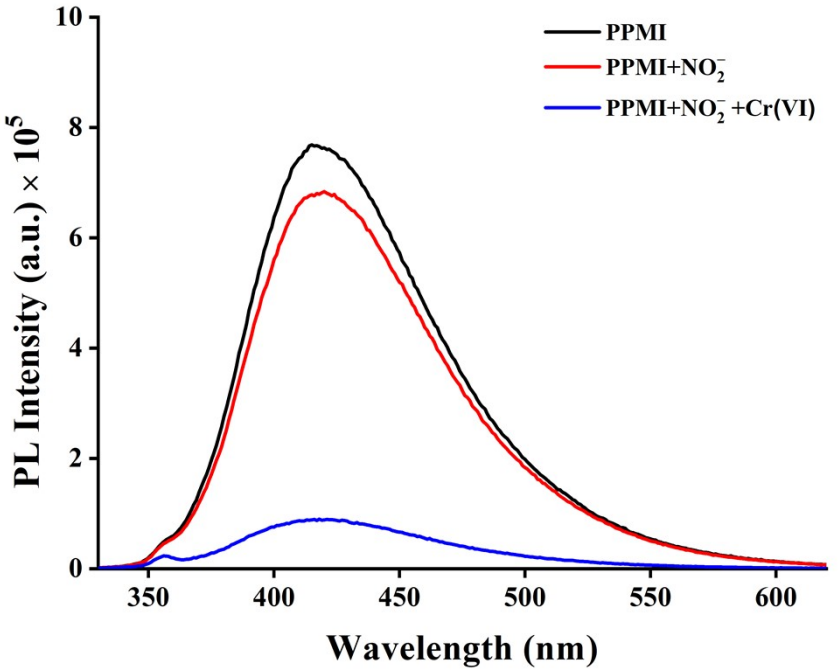

Fig. S25 Emission spectra of PPMI (black), PPMI in presence of NO_2^- (10 μM) (red), followed by addition of Cr(VI) (10 μM) (blue).

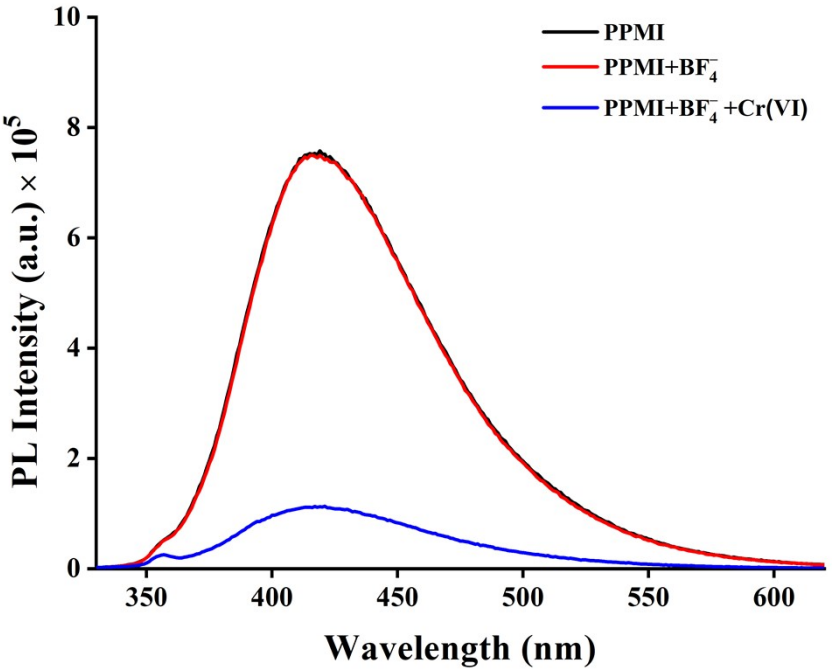

Fig. S26 Emission spectra of PPMI (black), PPMI in presence of BF_4^- (10 μM) (red), followed by addition of Cr(VI) (10 μM) (blue).

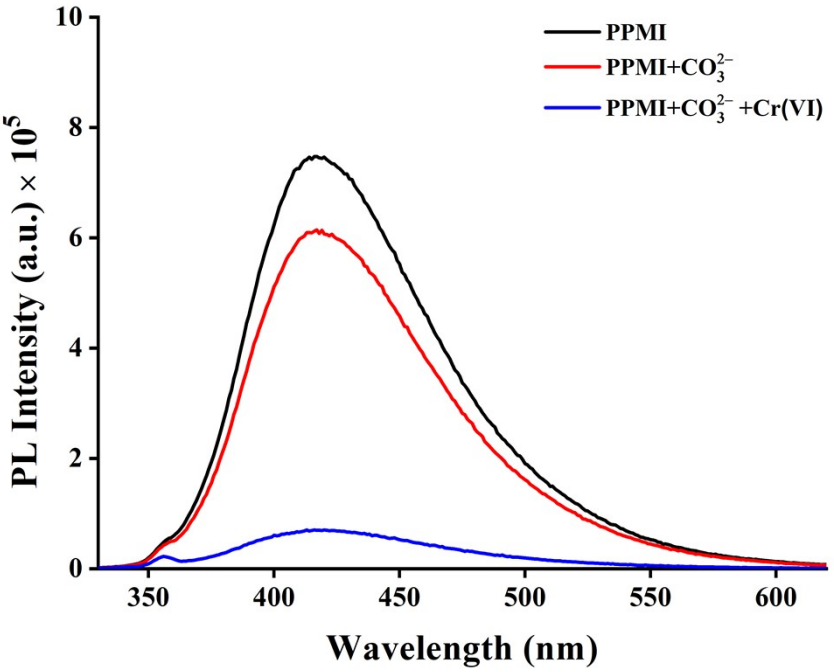

Fig. S27 Emission spectra of PPMI (black), PPMI in presence of CO_3^{2-} (10 μM) (red), followed by addition of Cr(VI) (10 μM) (blue).

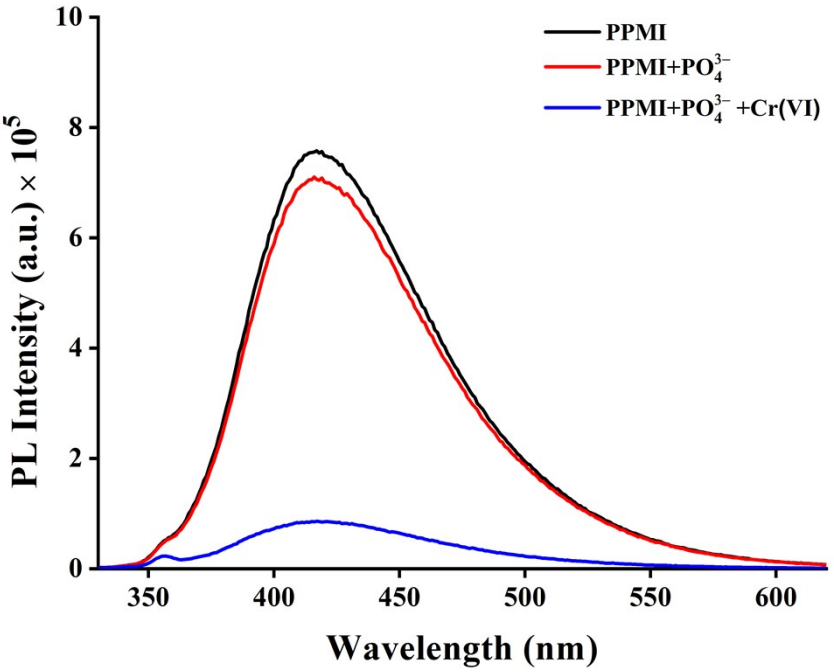

Fig. S28 Emission spectra of PPMI (black), PPMI in presence of PO_4^{3-} (10 μM) (red), followed by addition of Cr(VI) (10 μM) (blue).

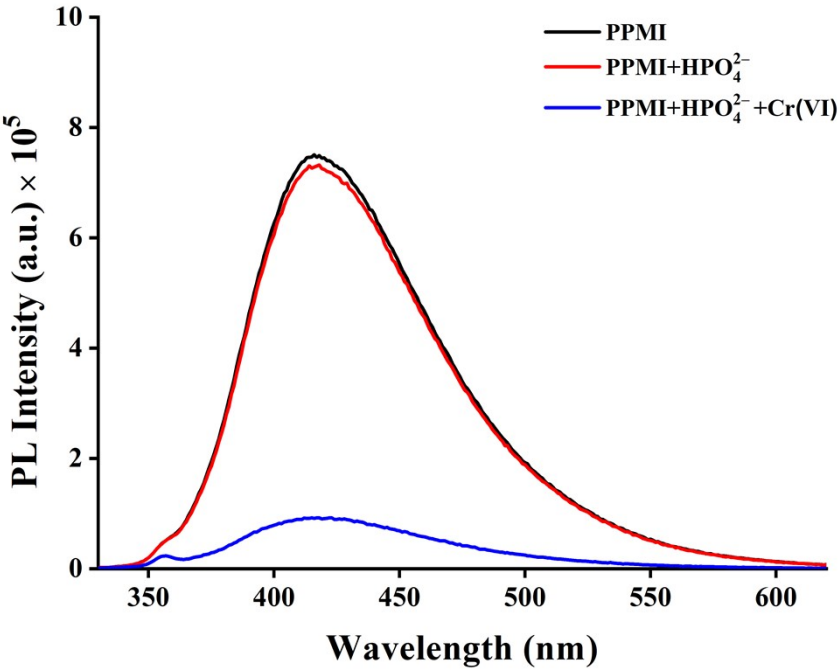

Fig. S29 Emission spectra of PPMI (black), PPMI in presence of HPO_4^{2-} (10 μM) (red), followed by addition of Cr(VI) (10 μM) (blue).

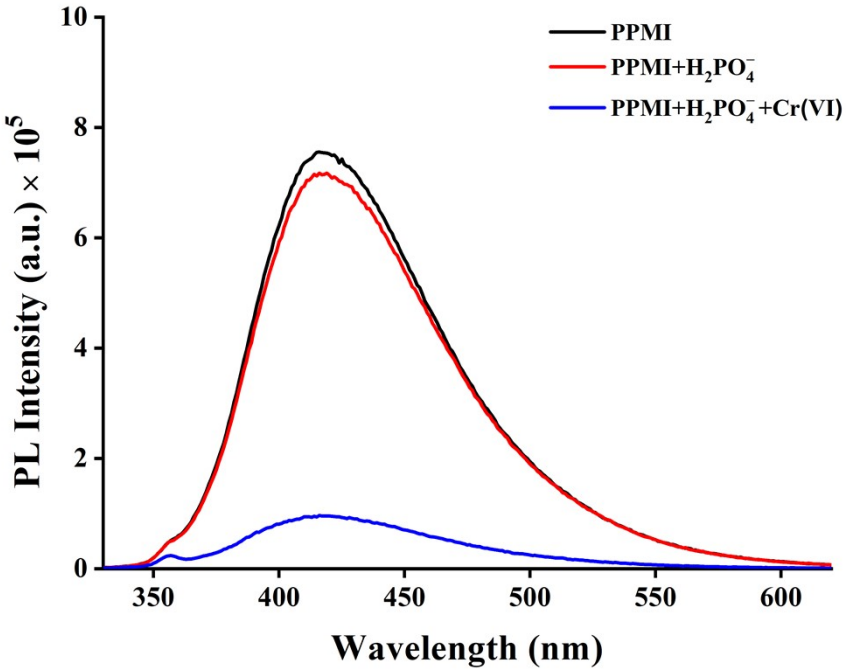

Fig. S30 Emission spectra of PPMI (black), PPMI in presence of $H_2PO_4^-$ (10 μM) (red), followed by addition of Cr(VI) (10 μM) (blue).

Table S3. Calculations for IFE corrections for quenching of PPMI by Cr(VI).

Cr(VI) (μM)	A_{ex}	A_{em}	I_{obs}	I_{corr}	I_{corr} /I_{obs} Correction factor (CF)	E_{obs}	E_{corr}
0	0.110057	0.008537	737813.1751	845752.7257	1.146296589	0	0
1	0.112169	0.010511	348499.2005	401367.1144	1.151701679	52.76593	52.54321
2	0.114876	0.013311	239672.1064	277786.4084	1.159026858	67.51588	67.15513
3	0.117624	0.015311	199720.9991	232750.8255	1.165379838	72.93068	72.48004
4	0.117805	0.015336	158308.7156	184533.5452	1.165656259	78.54352	78.18115
5	0.119372	0.015156	136513.9897	159382.6926	1.167519116	81.49749	81.15493
6	0.120572	0.015622	123761.5528	144771.3918	1.169760629	83.2259	82.88254
7	0.120755	0.01497	107523.0151	125708.2945	1.16912918	85.4268	85.13652
8	0.12165	0.015491	97319.72742	113964.9709	1.171036684	86.80971	86.52502
9	0.121675	0.015306	91008.45298	106554.6071	1.170820991	87.66511	87.40121
10	0.123496	0.015998	82843.89113	97276.39986	1.174213313	88.7717	88.49825

References:

1. M. A. S. Salem, A. M. Khan, Y. K. Manea, H. A. M. Saleh and M. Ahmad, *ACS Omega*, 2023, **8**, 1220-1231.
2. S. Menon, S. P. Usha, H. Manoharan, P. V. N. Kishore and V. V. R. Sai, *ACS Sens.*, 2023, **8**, 684-693.
3. X. Jiang, C. Tang, Z. Zhao, Y. Liao, J. Zhao, J. Hu, H. Zhang, Q. Yu, P.-L. Tremblay and T. Zhang, *ACS Sustainable Chem. Eng.*, 2023, **11**, 6610-6618.
4. M. Feng, X. Chen, Y. Liu, Y. Zhao, P. G. Karmaker, J. Liu, Y. Wang and X. Yang, *J. Mater. Chem. B*, 2023, **11**, 4020-4027.
5. M. Liu, S. Zhang, Y. Wang, J. Liu, W. Hu and X. Lu, *Anal. Chem.*, 2022, **94**, 1669-1677.
6. Y. Zhang, Y. Liu, F. Huo, B. Zhang, W. Su and X. Yang, *ACS Appl. Nano Mater.*, 2022, **5**, 9223-9229.
7. S. Bhatt, G. Vyas and P. Paul, *ACS Omega*, 2022, **7**, 1318-1328.
8. S. C. Pal, D. Mukherjee and M. C. Das, *Inorg. Chem.*, 2022, **61**, 12396-12405.
9. F. Li, G. Zhang, L. Zou, X. Zhang, F. Liu, H. Li, J. Xu and X. Duan, *ACS Appl. Polym. Mater.*, 2022, **4**, 815-821.
10. P. Ravichandiran, D. S. Prabakaran, N. Maroli, A. R. Kim, B.-H. Park, M.-K. Han, T. Ramesh, S. Ponpandian and D. J. Yoo, *J. Hazard. Mater.*, 2021, **419**, 126409.
11. L. Qiu, Z. Ma, P. Li, X. Hu, C. Chen, X. Zhu, M. Liu, Y. Zhang, H. Li and S. Yao, *J. Hazard. Mater.*, 2021, **419**, 126443.
12. W. Shi, M. He, W. Li, X. Wei, B. Bui, M. Chen and W. Chen, *ACS Appl. Nano Mater.*, 2021, **4**, 802-810.
13. S. Roy, S. Bardhan, D. Mondal, I. Saha, J. Roy, S. Das, D. K. Chanda, P. Karmakar and S. Das, *Sens. Actuators B Chem.*, 2021, **348**, 130662.
14. S. Roy, S. Bardhan, D. K. Chanda, J. Roy, D. Mondal and S. Das, *ACS Appl. Mater. Interfaces*, 2020, **12**, 43833-43843.
15. J. Sun, P. Guo, M. Liu and H. Li, *J. Mater. Chem. C*, 2019, **7**, 8992-8999.
16. Y. B. Yin, C. L. Conrad, K. N. Heck, F. Lejarza and M. S. Wong, *ACS Appl. Mater. Interfaces*, 2019, **11**, 17491-17500.
17. P. Li, X.-M. Yin, L.-L. Gao, S.-L. Yang, Q. Sui, T. Gong and E.-Q. Gao, *ACS Appl. Nano Mater.*, 2019, **2**, 4646-4654.
18. J. Song, H. Zhou, R. Gao, Y. Zhang, H. Zhang, Y. Zhang, G. Wang, P. K. Wong and H. Zhao, *ACS Sens.*, 2018, **3**, 792-798.
19. X. Shen, X. Yang, C. Su, J. Yang, L. Zhang, B. Liu, S. Gao, F. Gai, Z. Shao and G. Gao, *J. Mater. Chem. C*, 2018, **6**, 2088-2094.
20. B.-B. Lu, W. Jiang, J. Yang, Y.-Y. Liu and J.-F. Ma, *ACS Appl. Mater. Interfaces*, 2017, **9**, 39441-39449.
21. X.-Y. Guo, F. Zhao, J.-J. Liu, Z.-L. Liu and Y.-Q. Wang, *J. Mater. Chem. A*, 2017, **5**, 20035-20043.